Dynamics of β-Carotene-to-Chlorophyll Singlet Energy Transfer in the Core of Photosystem II

Frank L. de Weerd,* Jan P. Dekker, and Rienk van Grondelle

Department of Biophysics and Physics of Complex Systems, Division of Physics and Astronomy, Faculty of Sciences, Vrije Universiteit, De Boelelaan 1081, 1081 HV Amsterdam, The Netherlands

Received: December 16, 2002; In Final Form: April 4, 2003

The core of photosystem II comprises three major subcomplexes: the photochemical reaction center (RC) and the core antennas CP43 and CP47. All contain β-carotene as the only carotenoid, but the quantum efficiency of β-carotene-to-chlorophyll singlet energy transfer in the CP43, CP47, and RC complexes is poor. From a femtosecond transient absorption study of the isolated subcomplexes following β-carotene excitation, we show that mainly the β-carotene S_2 ($1B_u^+$) state is involved in the energy-transfer process. At most, a minor amount of energy transfer from "hot" β-carotene S_1 ($2A_g^-$) states is present in CP43 and CP47, but this S_1 contribution is absent in the RC. In all complexes, the relaxed S_1 state is not participating in energy transfer. This absence of energy transfer from S_1 states explains the low overall yield of β-carotene-to-chlorophyll singlet energy transfer in the PSII core.

Introduction

Carotenoids (Cars) play an important role in photosynthesis: On one hand, they quench singlet oxygen and chlorophyll (Chl) triplets (that can lead to the formation of singlet oxygen), and on the other hand, they harvest sunlight in a spectral region where Chls do not absorb. In the photosynthetic apparatus of higher plants, β-carotene is the only carotenoid species bound to the core complexes (reaction center (RC) and core antenna) of photosystem I (PSI) and photosystem II (PSII). In both photosystems, excitation energy is transferred via the core antennas to the RC, where an ultrafast charge separation (on the order of picoseconds) is initiated.[1,2]

This study concerns singlet energy transfer from the β-carotenes to the chlorins in the isolated subcomplexes of the PSII core: CP43, CP47, and the RC. The PSII core antenna proteins CP43 and CP47 each bind ∼2 β-carotenes and ∼15 Chls *a*, and the RC of PSII binds 2 β-carotenes, 6 Chls *a*, and 2 pheophytins *a*. In the RC, two β-carotene transitions that are differently oriented have been identified. One with a 0−0 transition at 506 nm lies "in the membrane plane", and the other with a 0−0 transition at 490 nm is "sticking out of the membrane plane" (77 K).[3] The two β-carotenes in the PSII RC are most likely excitonically coupled.[4,5]

In purple bacteria, Cars favor the all-trans form in the antenna proteins LH1 and LH2,[6] and the 15-*cis*-Car is selected by the photosynthetic reaction centers.[7] In the PSI core, 16 β-carotenes were modeled as all-trans, whereas 5 β-carotenes adopted a variety of configurations containing 1 or 2 cis bonds.[8] For the various complexes in the PSII core, this issue has not yet been completely settled. HPLC measurements on the RC gave contradictory results,[9,10] though results from Raman spectroscopy favor an all-trans configuration.[11,12] Located close to each other on one side of the RC complex, one β-carotene was modeled as an all-trans, and one, as a cis type in the crystal structure of PSII from *Synechococcus vulcanus*.[13] For the PSII core antenna protein CP47, the available information on the isomerization state of β-carotene points to an all-trans configuration.[14]

As with all Cars found in the photosynthetic apparatus, β-carotene has several low-lying excited singlet states: transitions between S_0 ($1A_g^-$, ground state) and S_1 ($2A_g^-$) are one-photon-forbidden, and the S_1 state generally becomes populated by internal conversion (IC) from higher states.[15] The energy of the β-carotene S_1 state is hardly influenced by the environment and is estimated to be at ∼700 nm, which is slightly lower than the lowest excited singlet state of Chl (∼680 nm).[16−18] The β-carotene S_1 state has a lifetime of ∼10 ps in a range of solvents (see, for example, ref 19). The $S_0 \rightarrow S_2$ ($1B_u^+$) transition is one-photon-allowed and is responsible for the characteristic strong visible absorption of β-carotene (400−520 nm). Because of dispersive interactions, the solvent can shift the energy of the β-carotene S_2 state and therefore also change the S_2 lifetime (120−180 fs; see, for example, ref 19).

In the weak-coupling limit, the rate of excitation-energy transfer (EET) between pigments is proportional to the square of the interaction energy and to the overlap between the donor emission and the acceptor absorption (Förster energy transfer[20]). Both the Car $S_0 \rightarrow S_2$ and the Car $S_0 \rightarrow S_1$ transitions can exhibit a large Coulombic interaction with the Chl electronic transitions. The Car $S_0 \rightarrow S_2$ transition mainly through dipole−dipole coupling[21−23] and the Car $S_0 \rightarrow S_1$ transition, despite its forbidden nature, may show significant interaction due to contributions of higher-order terms in the multipole expansion of the transition charge density.[21−24] Although EET from the Car S_1 and S_2 states to the Chls has to compete with fast internal conversion, energy transfer from both states can be fast in photosynthetic antennas where the relevant energy levels are well positioned. The total quantum efficiency of the Car-to-Chl energy transfer can reach up to 100%.[15]

In the PSII core, EET from "hot" β-carotene S_1 states might play a role: in an earlier study of β-carotene, an ∼300 fs relaxation process in S_1 was observed, and it was proposed that such a process is present in most Cars.[25] Similar "relaxation"

* Corresponding author. E-mail: weerd@nat.vu.nl. Tel: (+31) 20 4447934. Fax: (+31) 20 4447999.

10.1021/jp027737q CCC: $25.00
Published on Web 05/24/2003

phenomena were observed in the LH2 complex of *Rhodobacter sphaeroides*.[26] Recently, it was suggested that the transient population of hot Car S_1 states in LHCII gives rise to multiphasic EET to Chls on subpicosecond time scales.[27,28]

In an earlier study of EET in CP43 and CP47, we showed that energy equilibration at 77 K within the Chl Q_y bands takes place in 0.2−0.4 and 2−3 ps, thereby populating red-shifted states at 682−683 nm. The red state at 690 nm in CP47 is populated by an additional step of ∼17 ps.[29] The (lowest) electronic states in CP47 were further characterized by Chang et al.[30] and de Weerd et al.;[31] the spectroscopic properties of the several Chl pools in CP43 were characterized by Groot et al.[32] and Jankowiak et al.[33]

Inferred from excitation spectra, earlier studies have shown a poor efficiency of β-carotene-to-Chl singlet energy transfer in CP43, CP47, and the PSII RC (see below).[3,34,35] As of yet, however, no information about time scales and singlet excited states that are active in the transfer process is available. In this work, we present subpicosecond transient absorption spectra of isolated CP43, CP47, and PSII RC complexes. We conclude that in all three complexes mainly the β-carotene S_2 ($1B_u^+$) state acts as the donor state in the Car-to-Chl energy-transfer process. In CP43 and CP47, possibly a small amount of energy transfer occurs via hot S_1 states.

Experimental Section

Sample Preparation. CP43 and CP47−RC complexes were purified from spinach using the nonionic detergent *n*-dodecyl β,D-maltoside (β-DM).[32,36] CP47 was isolated from the CP47−RC complex as described elsewhere.[37] The reaction center of photosystem II, called D1-D2-cytochrome *b*559 (PSII RC), was isolated from the CP47−RC complex by means of a short Triton X-100 treatment.[34,38] CP47 and RC samples were dissolved in a buffer containing 0.03% (w/v) β-DM, 20 mM NaCl, and 20 mM BisTris (pH 6.5); in the case of CP43, BisTris was replaced by Hepes (pH 7.5). Prior to the transient absorption experiments, 10 μL of catalase (120 μg/mL), 50 μL of glucose (10 mM), and 10 μL of glucose oxidase (120 μg/mL) were added in this order to 70 μL of a buffer containing the RC particles such that the optical density in the Q_y maximum was 0.3−0.4 over the 1 mm path length of the cuvette. For the 77 K fluorescence excitation experiments on CP43 and CP47, 65% (v/v) glycerol was included in the buffer, and the β-DM concentration was raised to 0.09% (w/v). These samples were cooled to 77 K in a nitrogen reservoir cryostat (Oxford).

Excitation Spectra. Room-temperature (RT) and 77 K fluorescence excitation spectra were measured on a homebuilt fluorometer. Vertically polarized excitation light was provided by a tungsten−halogen lamp in combination with a Chromex 500SM spectrograph (length 0.5 m) and was modulated by a mechanical chopper. Fluorescence (passing through a high-pass filter and a polarizer set to the magic angle) was collected at right-angle geometry using a photomultiplier and subsequently led to a lock-in amplifier. The transmission of the sample was measured simultaneously using a photodiode. Calibration of the setup for the wavelength-dependent intensity of the excitation light was performed using three different laser dyes.

Transient Absorption. Absorption difference spectra were recorded with a femtosecond spectrophotometer, described in detail elsewhere.[39] In short, the output of a Ti:sapphire oscillator was amplified by means of chirped pulse amplification (Alpha-1000 US, B. M. Industries) generating 100 Hz, 800 nm, 60 fs pulses. Single-filament probe white light was generated in a 2 mm sapphire plate. To minimize the chirp, parabolic reflectors were used to recollimate and focus the probe light in the sample. Pump pulses were centered at either ∼400 or ∼510 nm. Pump light at ∼400 nm was obtained by doubling the ∼800 nm fundamental (∼10 nJ/pulse); pulses around 510 nm were produced in a homebuilt, noncollinear optical parametric amplifier,[40] and a 12 nm (fwhm) bandwidth was obtained after prism compression down to ∼40 fs (∼40 nJ/pulse). The magic angle spectra were obtained by rotating the polarization of the pump with a Berek polarization compensator (New Focus, 5540). Time-gated spectra were recorded with a homebuilt camera consisting of a double diode array read out at the laser frequency (100 Hz). Typically, 800 difference absorbance spectra were averaged per delay. The chopper frequency was set such that the excitation beam was blocked every other shot. As a result, the sample was excited every 20 ms. The cuvette (1 mm path length) was shaken to refresh the sample from shot to shot. The dispersion curve and instrument response width were characterized by measuring the optical Kerr effect in water.

Degradation of the sample is a concern especially for the PSII RC because of photodamage after charge separation. However, steady-state absorption spectra were measured before and after the experiment, and these were virtually identical in all cases. Further exposure of the RC samples to extensive laser illumination resulted in a 1 nm blue shift of the Chl/pheophytin Q_y absorption maximum, indicating that damage to the RC sample did occur in the long run.

Analysis of Transient Absorption Data. The spectra were fitted with a global analysis fitting program.[41] A sequential model with increasing lifetimes was assumed where each species evolves into the next one. Note that these species-associated difference spectra (SADS) are not necessarily associated with "pure states" and are used as a way to describe the time evolution present in the data. Dispersion within the probe continuum (measured as the optical Kerr effect in water) was fitted with a third-order polynomial. The dispersion was almost absent in the spectral region from 650 to 720 nm (at most ∼20 fs), whereas a dispersion of ∼3 fs/nm was obtained down to 470 nm. The instrument response width is mainly determined by the uncompressed white light and was fitted from the Kerr measurements in water assuming a Gaussian function. The obtained width (fwhm) varied from 140 fs at ∼470 nm to 80 fs at ∼700 nm.

Fluorescence Excitation Results

Inferred from excitation spectra, it has been established that only a limited amount of singlet energy transfer from the β-carotenes to the Chls takes place in the PSII core. Values for the quantum efficiency of <20% at 4 K[3] and of 30% at 77 K[34] have been reported for the PSII RC. A value of 40% at 4 K has been reported for CP47.[3] Alfonso et al. report a low efficiency of Car-to-Chl EET in CP43 and CP47.[35] We note also that the quantum yield of triplet energy transfer is low: about 50% of the Chl triplets are quenched by the Cars in CP43[32] and CP47[37] at 4 K.

In this work, we have also measured the fluorescence excitation spectra for the isolated PSII core antenna complexes CP43 and CP47 at RT and 77 K, and these spectra are shown (solid lines) in Figure 1 (CP43) and Figure 2 (CP47). The fluorescence was detected through a high-pass filter (>600 nm). From a comparison with the $1-T$ spectra normalized in the Chl Soret region (dashed lines), it follows that the total efficiency of EET from β-carotene to Chl in all cases equals ∼35%, in line with the literature reports mentioned above. In the next section, we will establish which electronic states are involved

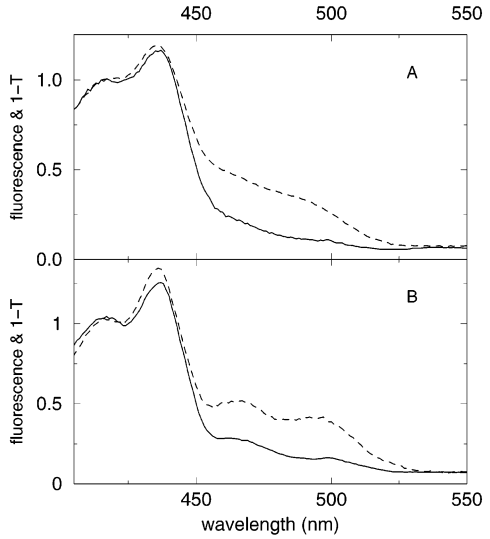

Figure 1. Fluorescence excitation (—) and 1−*T* spectra (- - -) of CP43 at (A) RT and at (B) 77 K.

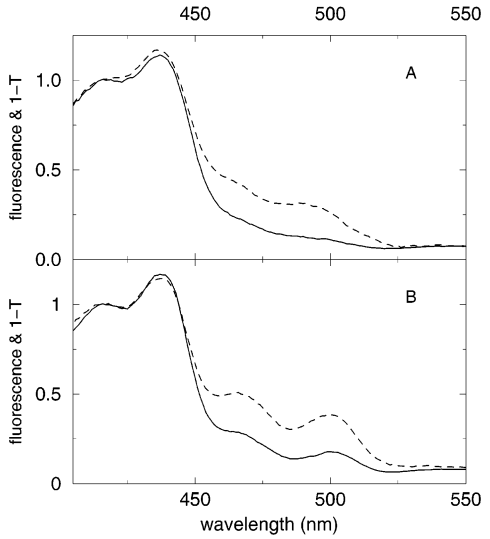

Figure 2. Fluorescence excitation (—) and 1−*T* spectra (- - -) of CP47 at (A) RT and at (B) 77 K.

in this energy transfer process, and why the efficiencies are lower compared to the values for many other photosynthetic pigment−protein complexes.

Transient Absorption Results

Excited-state dynamics in the isolated subcomplexes of the PSII core (CP43, CP47, and RC) were measured at RT. First, we consider the possibility of Chl triplet accumulation in these experiments. RC triplets decay (between 40 and 200 K) with time constants between 1 and 2 ms.[42] At 270 K, a 1.0 ms lifetime was observed.[43,44] Chl triplets in CP43[32] and CP47[37] decay (at 4 K) with time constants on the order of 1−3 ms. Most likely, a millisecond lifetime will also be observed at RT. In this work, the samples were excited every 20 ms, thus avoiding the accumulation of Chl triplet states. For CP43 and CP47, experiments were performed using two excitation wavelengths: ∼510 nm, exciting almost exclusively β-carotene, and ∼400 nm, exciting Chl almost exclusively. For the RC, only the 510 nm excitation, which preferentially excites the red-most β-carotene transition in the PSII RC, was used. In all cases, absorption difference spectra were recorded between 470 and 720 nm and for pump−probe delays up to ∼4 ns.

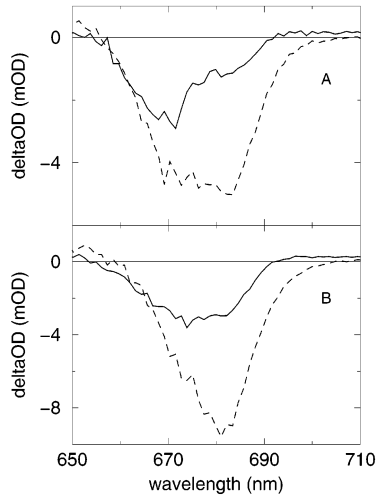

Figure 3. Absorption difference spectra at pump−probe delays of 0.0 ps (—) and 0.5 ps (- - -) in the Chl Q_y region at RT in (A) CP43 and (B) CP47 after 400 nm excitation. The pump and probe were at the magic angle. No wavelength-dependent time-zero correction was performed because the total dispersion over this spectral region is only ∼20 fs.

Transient Absorption upon 400 nm Excitation. First, we will discuss the spectral evolution in the 650−720 nm probe region, followed by that in the 470−650 nm region. Absorption difference spectra in the Chl Q_y region (650−720 nm) at pump−probe delays of 0.0 (solid lines) and 0.5 ps (dashed lines) after excitation at 400 nm are shown in Figure 3A (CP43) and B (CP47). The spectra at 0.0 ps can be assigned to the bleaching of the Chl Q_y state due to excitation at 400 nm into the Chl Soret band. Consequently, because of relaxation from Soret to Q_y on a time scale faster than 0.5 ps, the amplitudes of the integrated spectra approximately double because of the addition of stimulated emission (SE) from the Q_y states. Part of the red shift observed between 0.0 and 0.5 ps must be due to fast equilibration within the Q_y band. On a few picoseconds time scale, a minor spectral evolution associated with further energy equilibration is observed, followed by a decay on a few nanoseconds time scale (not shown). These results compare well with the fast equilibration within the Q_y band (<0.5 ps and a few picoseconds) observed for CP43 and CP47 at 77 K.[29] In the 470−650 nm region, the Chls display only a small ESA; therefore, mainly the Cars, which absorb a small amount of the 400 nm pump pulses (though much less than Chl), contribute to the transient absorption in this spectral region. Though much smaller (maximum 1.5 mOD at ∼560 nm), these dynamics (not shown) are similar to those observed for CP43 and CP47 upon exciting the Cars at 510 nm (see below).

Transient Absorption upon 510 nm Excitation. The same experiment was performed for CP43, CP47, and the RC using 510 nm excitation. At this excitation wavelength, Chl hardly absorbs, and β-carotene is excited almost exclusively. Pheophytin, however, possesses an absorption band at ∼510 nm,[38] and as a result, a minor amount of pump-pulse absorption in the RC experiment is due to pheophytin. Still, a majority of the absorption is due to the "red" Car transition. Because of the scatter of the pump pulses present in the data, the 485−530 nm region was not taken into account. Before we discuss the spectral region to the blue of the scatter (the Car S_2 bleach), we will first present the results obtained in the region to the red of the scatter (the Car S_2 SE, the Car $S_1 \rightarrow S_N$ ESA, and the Chl Q_y bleaching/SE).

530−720 nm Probe. In Figure 4 , we show a few experimentally observed traces (solid lines) at representative wave-

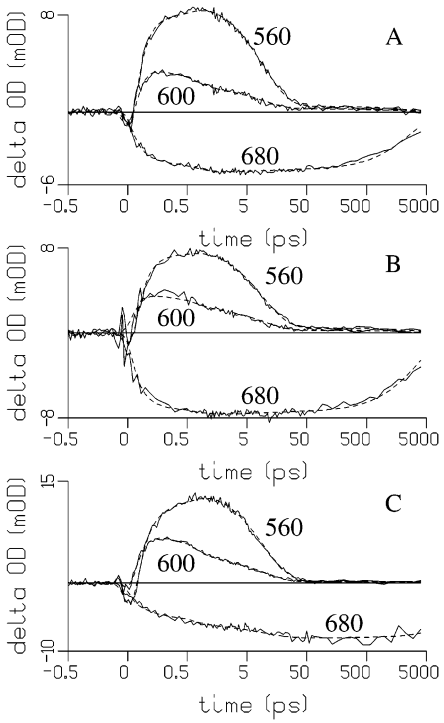

Figure 4. Experimentally observed traces probed at 560, 600, and 680 nm (—) and global analysis fit (- - -) of (A) CP43, (B) CP47, and (C) the RC at RT with 510 nm excitation. A wavelength-dependent time-zero correction was performed to account for the dispersion present in the data (see text). The pump and probe were at the magic angle. Note that the time axis is linear between −0.5 and +0.5 ps and logarithmic at later delay times.

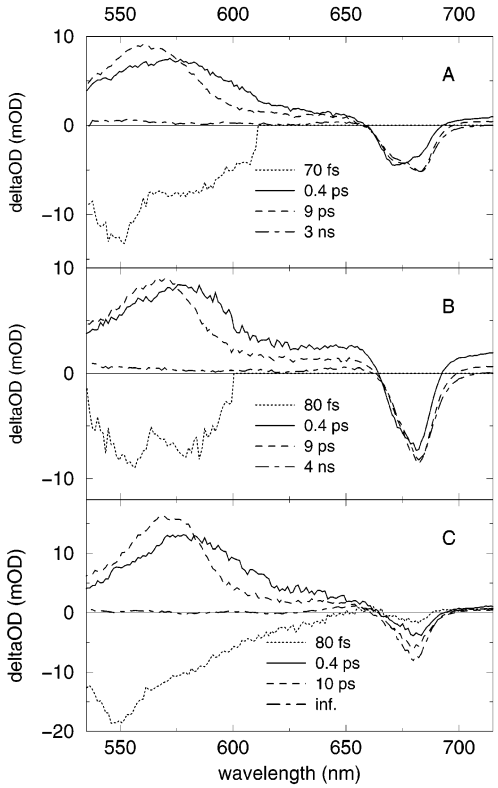

Figure 5. Global analysis SADS of (A) CP43, (B) CP47, and (C) the RC corresponding to the global fits in Figure 4 (RT with 510 nm excitation). Each species evolves with the given time constant into the next one. The first SADS (···) was set to zero above 610 nm (CP43) and 600 nm (CP47). See the text.

lengths (560, 600, and 680 nm). In the 530−620 nm region, an instantaneous SE from the Car S_2 states is followed by a large Car ESA that is decaying completely on an ∼10 ps time scale. At 680 nm, bleaching/SE from the Chl Q_y states is growing in because of energy transfer from the Cars. These signals decay on a few nanoseconds time scale (CP43 and CP47), whereas the RC signal does not decay on the time scale of our experiment because of charge separation.

In all of the complexes, the spectral evolution was fit to a sequential model, and typically four species with increasing lifetimes were required for a good fit. These global fits are also shown in Figure 4 (dashed lines). In CP47 (Figure 4B), in the 530−630 nm region, a cross-phase modulation was present around time zero. With this exception, the global fits represent a good description of all of the measured traces. The four species-associated difference spectra (SADS) that were required for each global fit are displayed in Figure 5.

The first SADS in each panel (instantaneous spectrum, dotted line) exhibits SE from the Car S_2 state. All transient signals in the Chl Q_y region were close to zero. (See, for instance, the traces probed at 680 nm in Figure 4.) To facilitate the analysis of the data in this region, the CP43 and CP47 instantaneous spectra (first SADS) were set to zero for wavelengths longer than 600−610 nm (because Chls are not directly excited). This was not done for the PSII RC because the pheophytin absorption band at ∼510 nm gives rise to some instantaneous bleaching of pheophytin Q_y states. The loss of the Car S_2 state and the arrival of excitations on the Car S_1 state and on the Chls is fitted with a rate constant of $(80 \pm 20\ \text{fs})^{-1}$. This rate constant reflects the sum of the Car $S_2 \rightarrow S_1$ IC and the Car $S_2 \rightarrow$ Chl energy-transfer rate constants.

The second SADS (solid line) clearly displays the Car $S_1 \rightarrow S_N$ ESA and the Chl bleaching/SE. The Car region of the spectra can be assigned to a hot S_1 state because further spectral evolution takes place: on a 0.4 ps time scale, the second SADS is replaced by the third SADS (dashed line). This spectral evolution (loss of red, gain of blue ESA) is characteristic for the β-carotene molecule: in different organic solvents, it was observed as a more or less conservative process (meaning that the integrated ESA does not change much in time) and can be ascribed to the cooling of vibrationally hot S_1 states. In ref 25, an alternative model involving the regeneration of all-trans Car molecules in S_1 after small distortions in S_2 was proposed. For CP47, the 0.4 ps process does not appear to be conservative (Figure 5B). Because of uncertainties in the global fits, we have investigated the possible decay of ESA on this time scale in a more direct manner by plotting the integrated absorption as a function of pump−probe delay. The thus-integrated spectra do not show an appreciable decay on an ∼0.4 ps time scale (not shown). Note that the Car $S_1 \rightarrow S_N$ ESA overlaps the Chl Q_y region and extends all the way up to 720 nm. Therefore, the observed spectral dynamics in the Chl Q_y region are a mixture of Chl equilibration and the relaxation in the Car S_1 state. We note that the time constant of 0.4 ps is mainly fitted from the broad Car region of the spectrum rather than from the narrow Chl contribution. The relaxation within the Chl Q_y band will be discussed in more detail below.

The third SADS, associated with the relaxed Car S_1 state and equilibrated Chl pool, displays an absorption maximum for CP43 at ∼562 nm, for CP47 at ∼568 nm, and for the RC at ∼570 nm. The transition from the third to the fourth SADS (dotted−dashed line) occurs with a 9−10 ps time constant ($S_1 \rightarrow S_0$ IC), which is similar to the $S_1 \rightarrow S_0$ IC time in solution.

The fourth SADS can be associated with the equilibrated Chl pool. The spectra display bleaching/SE in the Q_y region and a

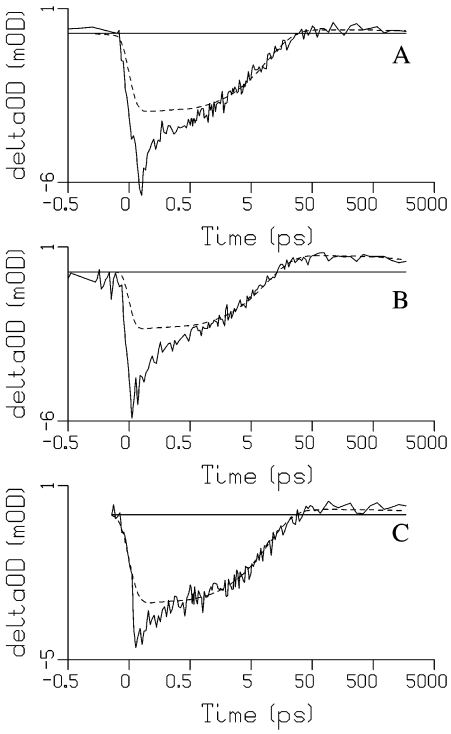

Figure 6. Experimentally observed traces (—) in (A) CP43, (B) CP47, and (C) the PSII RC probed around 475 nm after 510 nm excitation. The pump and probe were at the magic angle. Dashed lines represent a single-exponential decay with time constants resulting from the global fits in Figures 4 and 5. Note that the time axis is linear between −0.5 and +0.5 ps and logarithmic at later delay times.

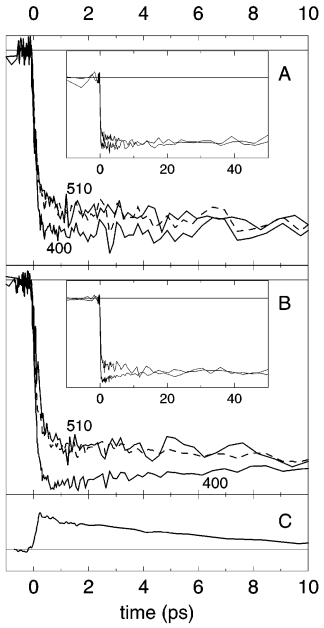

Figure 7. Difference absorption integrated over 655−705 nm as a function of the pump−probe delay (—) of (A) CP43 after excitation at 400 and 510 nm, (B) CP47 after excitation at 400 and 510 nm, and (C) β-carotene in benzyl alcohol after excitation at 475 nm.[25] A wavelength-dependent time-zero correction was made in panel C because of the greater amount of dispersion in these data. The signal of β-carotene in benzyl alcohol could be scaled such that for CP43 and CP47 the sum (- - -) with the signals after 400 nm excitation more or less reproduces the signals after 510 nm excitation.

small ESA in the 530−650 nm region. The CP43 and CP47 spectra decay to zero on a 3−4 ns time scale, whereas the RC spectrum does not decay for pump−probe delays up to 4 ns because of charge separation.

We emphasize that the β-carotene S_1 state in CP43, CP47, and the PSII RC has a lifetime similar to the one in solution (∼10 ps); therefore, we conclude that no significant EET from relaxed Car S_1 states to Chls takes place in the PSII core.

470−480 nm Probe. We will now consider the 470−480 nm region (blue from the scatter) covering the $S_0 \rightarrow S_2$ absorption band of β-carotene. All wavelengths covering this spectral window showed similar kinetics, and the traces (summed over a few wavelengths around 475 nm) are shown in Figure 6 (solid lines). The Chl Soret bleaching/SE (extending up to ∼460 nm) is absent in these traces. Because the Car S_2 state remains bleached upon IC to S_1, the dynamics in these signals follow the return of Car excited states to the ground state. In Figure 6, we have plotted single-exponential decays (dashed lines) fixed to 9−10 ps, which is the lifetime of the Car S_1 state resulting from the global fits in Figures 4 and 5. The amplitudes of these 9−10 ps decays were matched to the slow tail of the observed decays. Obviously, this slow loss of Car excited states results from IC to the ground state. The early-time residuals reflect the Car excited states loss due to EET to Chl plus possibly some SE from the Car S_2 states (especially in the first few tens of femtoseconds) and a small ingrowth of Chl ESA (especially pronounced for CP47). This Chl ESA contribution remains after the complete loss of Car excited states (Figure 6). From these traces, we can conclude the following: (i) The total EET efficiency for the RC is lower than for CP43 and CP47. The absolute efficiencies are difficult to retrieve from these traces because of the unknown contribution of SE from the Car S_2 states. (ii) An ∼90 fs component, reflecting the EET from the Car S_2 states, is present in all of the residuals, and the lifetime is similar to the Car S_2 excited state lifetimes obtained in Figures 4 and 5. For the RC, although the exact time constant is difficult to obtain because of a limited signal-to-noise ratio, this component is the only EET component. (No few hundred femtosecond time constant is present in the residuals.) For CP43 and CP47, however, a small ∼0.8 ps component is present in addition to the ∼90 fs component. Note the different deviations between the solid and dashed lines around 0.5 ps in Figure 6. Possibly, this slower component reflects EET from hot Car S_1 states.

Comparing the Arrival of Excitations on Chl with 400 and 510 nm Excitation. We have shown that hot β-carotene S_1 states exist for a few hundred femtoseconds not only in organic solvents but also in protein environments such as CP43, CP47, and the RC. Furthermore, the loss of Car S_2 bleaching (monitoring the return of Car excited states to the ground state) suggests a small amount of energy transfer from hot S_1 states on a 0.5−1.0 ps time scale in CP43 and CP47. This should give rise to an increase in the bleaching/SE in the Chl Q_y region for the same time scale. In the global analysis in Figures 4 and 5, this increase might be obscured by Q_y spectral relaxation and perhaps annihilation. To investigate the possible extent of this hot S_1 energy transfer in CP43 and CP47, we have chosen the following approach:

The integrated spectrum over the 655−705 nm region as a function of the pump−probe delay is displayed for CP43 (Figure 7A) and CP47 (Figure 7B). The total dispersion over this spectral window equals ∼20 fs and therefore does not greatly influence any observations on the time scale of a few hundred femtoseconds or longer. We emphasize that no scaling of the signals upon 400 and 510 nm excitation was performed. The conditions were chosen such that the same number of excitations is present in the antenna at later delay times.

Upon 400 nm excitation, the time-zero signal is a bleaching on an ~100 fs time scale followed by the addition of SE (Figure 3). The signal observed in CP43 does not decay on a subpicosecond time scale, suggesting that no appreciable annihilation takes place. In contrast to the kinetics observed in CP43, the signal in CP47 decreases on a few picoseconds time scale, which can be ascribed to the red (excitonic) states having a lower oscillator strength than the initially excited states at ~670 nm. A similar but more pronounced observation was made for CP47 at 77 K.[29] For CP43 and CP47, upon 510 nm excitation, the signals display an initially fast ingrowth of bleaching/SE due to transfer from Car S_2 states, followed by a slow rise component of 0.5−1.0 ps. To estimate the amount of hot S_1 energy transfer in these traces, we must investigate the contribution to this signal caused by the loss of Car $S_1 \rightarrow S_N$ ESA. Note that the Car $S_1 \rightarrow S_N$ ESA extends up to 720 nm; consequently, the subpicosecond relaxation in the Car S_1 state is also present in the Q_y spectral region (Figure 5). To quantify the contribution due to the loss of Car $S_1 \rightarrow S_N$ ESA in the increase of the integrated signal in the Chl Q_y region after 510 nm excitation, we also present the signal of β-carotene in benzyl alcohol integrated over 655−705 nm (Figure 7C).[25] The sum of this trace and the traces after 400 nm excitation (represented by the dashed lines) more or less reproduces the traces upon 510 nm excitation for CP43 as well as for CP47. Therefore, judging from the transient absorption in the Chl Q_y region, we estimate that energy transfer from hot Car S_1 states is only a small fraction of the total in CP43 and CP47. We conclude that almost all Car-to-Chl transfer takes place on an ~100 fs time scale (from S_2).

Discussion

In this work, we show for the first time subpicosecond transient absorption in isolated CP43, CP47, and RC complexes following Car excitation. We are able to describe the dynamics of the low-efficiency Car-to-Chl EET. The roles that the various Car excited states, S_2, hot S_1, and S_1 play in the energy-transfer process are discussed below.

Transfer from the Car S_2 States. A vast majority of the transfer originates from the β-carotene S_2 state. Efficient transfer follows from the large spectral overlap between the Car S_2 emission and the Chl Q_x and/or vibronic Q_y absorption and the dipole−dipole coupling between these states. The yield of this transfer does not exceed ~35% because of the competing $S_2 \rightarrow S_1$ IC. Although the observed Car S_2 lifetime in the PSII RC is similar to those in CP43 and CP47, uncertainties in the fast times of the global fits allow for a lower yield as inferred from the S_2 bleaching kinetics in Figure 6. We also note that most likely only one of the two Cars in the RC is seen in this experiment if the red-most transition of two (probably) weakly coupled Cars is excited at 510 nm.[5]

When neglecting a possible minor amount of transfer from other states (hot S_1), we can combine the Car S_2 loss τ_{S_2} ($k_{S_2}^{-1}$) for CP43 and CP47 with the yield (η) inferred from the excitation spectra (~0.35) to calculate the $S_2 \rightarrow S_1$ IC time τ_{IC} (k_{IC}^{-1}):

$$\eta = \frac{k_{ET}}{k_{S_2}} = \frac{k_{ET}}{k_{ET} + k_{IC}} \quad (1)$$

k_{ET} is the intrinsic rate of energy transfer to Chl. The internal conversion time τ_{IC} will then equal $\tau_{S_2}/(1 - \eta) = 120 \pm 30$ fs. How does this time constant compare with suggested IC times in the literature? The PSII proteins represent a polarizable medium, as can be inferred from the downshifted S_2 energies of β-carotene. Given the narrow vibronic bands of β-carotene in the CP47 absorption spectrum, the CP47 protein was proposed to be nonpolar.[45] Using the refractive index reported by Renge et al. ($n = 1.51$)[45] and the relation S_2 lifetime versus polarizability for nonpolar media given by Macpherson et al.,[19] the expected IC time is 150 fs, which is close to the value of 120 ± 30 fs obtained here.

Transfer from Hot Car S_1 States. Despite the forbidden nature of the Car $S_0 \rightarrow S_1$ transition, transfer to Chls from (hot) Car S_1 states may occur and can be explained by a coupling using higher-order terms in the multipole expansion of the transition charge density.[21−24] The transient population of hot Car S_1 states, together with the loss of Car S_2 bleaching on a 0.5−1.0 ps time scale, indeed suggests the presence of transfer from hot β-carotene S_1 states in CP43 and CP47. However, by plotting the integrated absorption as function of the pump−probe delay, this component could not easily be resolved as a loss of Car ESA nor as an increase of Chl bleaching/SE. We conclude that energy transfer from hot Car S_1 states is at most only a small fraction of the total.

More subpicosecond energy transfer from hot Car S_1 states is present in LHCII.[27,28] In those studies, the Car S_1 states were populated using two-photon excitation (TPE), thereby avoiding the involvement of the Car S_2 states. In the TPE experiment of LHCII, a rise of 250 ± 50 fs was seen in the Chl fluorescence. The observed spectrum (by scanning the TPE wavelength) was blue-shifted and more narrow than the TPE spectrum monitoring the Car $S_1 \rightarrow S_N$ ESA of lutein (the most abundant Car in LHCII) in solution, suggesting that only the higher-energy S_1 states transfer to Chls (on a subpicosecond time scale).

Transfer from the Relaxed Car S_1 States. The relaxed Car S_1 state seemed to be inactive in the Car-to-Chl EET process in CP43, CP47, and the PSII RC. Because energy transfer in the PSII core from hot Car S_1 states is at most only a small fraction of the total and is absent from relaxed Car S_1 states, this transfer is apparently very much limited by the coupling and/or by the spectral overlap between the Car S_1 emission and the Chl Q_y absorption.

Acknowledgment. We thank Henny van Roon for the expert preparation of the CP43, CP47, and RC particles and Abdellatif Ouchchahd for assistance with the fluorescence excitation experiments. This research was supported by The Netherlands Organization for Scientific Research (NWO) via the Dutch Foundation for Earth and Life Sciences (ALW).

References and Notes

(1) van Grondelle, R.; Dekker, J. P.; Gillbro, T.; Sundström, V. *Biochim. Biophys. Acta* **1994**, *1187*, 1−65.

(2) Diner, B. A.; Babcock, G. T. In *Oxygenic Photosynthesis: The Light Reactions*; Ort, D. R., Yocum, C. F., Eds.; Kluwer Academic Publishers: Dordrecht, The Netherlands, 1996; pp 213−247.

(3) van Dorssen, R. J.; Breton, J.; Plijter, J. J.; Satoh, K.; van Gorkom, H. J.; Amesz, J. *Biochim. Biophys. Acta* **1987**, *893*, 267−274.

(4) Newell, W. R.; van Amerongen, H.; Barber, J.; van Grondelle, R. *Biochim. Biophys. Acta* **1991**, *1057*, 232−238.

(5) Frese, R. N.; Germano, M.; de Weerd, F. L.; van Stokkum, I. H. M.; Shkuropatov, A. Y.; Shuvalov, V. A.; van Gorkom, H. J.; van Grondelle, R.; Dekker, J. P. Submitted for publication.

(6) McDermott, G.; Prince, S. M.; Freer, A. A.; Hawthornthwaitelawless, A. M.; Papiz, M. Z.; Cogdell, R. J.; Isaacs, N. W. *Nature* **1995**, *374*, 517−521.

(7) de Groot, H. J. M.; Gebhard, R.; van der Hoef, I.; Hoff, A. J.; Lugtenburg, J.; Violette, C. A.; Frank, H. A. *Biochemistry* **1992**, *31*, 12446−12450.

(8) Jordan, P.; Fromme, P.; Witt, H.-T.; Klukas, O.; Saenger, W.; Krauss, N. *Nature* **2001**, *411*, 909−917.

(9) Bialek-Bylka, G. E.; Tomo, T.; Satoh, K.; Koyama, Y. *FEBS Lett.* **1995**, *363*, 137−140.

(10) Yruela, I.; Tomás, R.; Sanjuán, M. L.; Torrado, E.; Aured, M.; Picorel, R. *Photochem. Photobiol.* **1998**, *68*, 729−737.

(11) Ghanotakis, D. F.; de Paula, J. C.; Demetriou, D. M.; Bowlby, N. R.; Petersen, J.; Babcock, G. T.; Yocum, C. F. *Biochim. Biophys. Acta* **1989**, *974*, 44−53.

(12) Telfer, A.; Frolov, D.; Barber, J.; Robert, B.; Pascal, A. *Biochemistry* **2003**, *42*, 1008−1015.

(13) Kamiya, N.; Shen, J. R. *Proc. Natl. Acad. Sci. U.S.A.* **2003**, *100*, 98−103.

(14) de Paula, J. C.; Liefshitz, A.; Hinsley, S.; Lin, W.; Chopra, V.; Long, K.; Williams, S. A.; Betts, S.; Yocum, C. F. *Biochemistry* **1994**, *33*, 1455−1466.

(15) Frank, H. A.; Cogdell, R. J. *Photochem. Photobiol.* **1996**, *63*, 257−264.

(16) Haley, J. L.; Fitch, A. N.; Goyal, R.; Lambert, C.; Truscott, T. G.; Chacon, J. N.; Stirling, D.; Schalch, W. *J. Chem. Soc., Chem. Commun.* **1992**, *17*, 1175−1176.

(17) Andersson, P. O.; Bachilo, S. M.; Chen, R. L.; Gillbro, T. *J. Phys. Chem.* **1995**, *99*, 16199−16209.

(18) Onaka, K.; Fujii, R.; Nagae, H.; Kuki, M.; Koyama, Y.; Watanabe, Y. *Chem. Phys. Lett.* **1999**, *315*, 75−81.

(19) Macpherson, A. N.; Gillbro, T. *J. Phys. Chem. A* **1998**, *102*, 5049−5058.

(20) Förster, Th. In *Modern Quantum Chemistry*; Sinanoglu, O., Ed.; Academic Press: New York, 1965; Part 2, pp 93−137.

(21) Krueger, B. P.; Scholes, G. D.; Jimenez, R.; Fleming, G. R. *J. Phys. Chem. B* **1998**, *102*, 2284−2292.

(22) Krueger, B. P.; Scholes, G. D.; Fleming, G. R. *J. Phys. Chem. B* **1998**, *102*, 5378−5386.

(23) Damjanovic, A.; Ritz, T.; Schulten, K. *Phys. Rev. E* **1999**, *59*, 3293−3311.

(24) Hsu, C. P.; Walla, P. J.; Head-Gordon, M.; Fleming, G. R. *J. Phys. Chem. B* **2001**, *105*, 11016−11025.

(25) de Weerd, F. L.; van Stokkum, I. H. M.; van Grondelle, R. *Chem. Phys. Lett.* **2002**, *354*, 38−43.

(26) Papagiannakis, E.; Kennis, J. T. M.; van Stokkum, I. H. M.; Cogdell, R. J.; van Grondelle, R. *Proc. Natl. Acad. Sci. U.S.A.* **2002**, *99*, 6017−6022.

(27) Walla, P. J.; Yom, J.; Krueger, B. P.; Fleming, G. R. *J. Phys. Chem. B* **2000**, *104*, 4799−4806.

(28) Walla, P. J.; Linden, P. A.; Ohta, K.; Fleming, G. R. *J. Phys. Chem. A* **2002**, *106*, 1909−1916.

(29) de Weerd, F. L.; van Stokkum, I. H. M.; van Amerongen, H.; Dekker, J. P.; van Grondelle, R. *Biophys. J.* **2002**, *82*, 1586−1597.

(30) Chang, H. C.; Jankowiak, R.; Yocum, C. F.; Picorel, R.; Alfonso, M.; Seibert, M.; Small, G. J. *J. Phys. Chem.* **1994**, *98*, 7717−7724.

(31) de Weerd, F. L.; Palacios, M. A.; Andrizhiyevskaya, E. G.; Dekker, J. P.; van Grondelle, R. *Biochemistry* **2002**, *41*, 15224−15233.

(32) Groot, M. L.; Frese, R. N.; de Weerd, F. L.; Bromek, K.; Pettersson, Å.; Peterman, E. J. G.; van Stokkum, I. H. M.; van Grondelle, R.; Dekker, J. P. *Biophys. J.* **1999**, *77*, 3328−3340.

(33) Jankowiak, R.; Zazubovich, V.; Rätsep, M.; Matsuzaki, S.; Alfonso, M.; Picorel, R.; Seibert, M.; Small, G. J. *J. Phys. Chem. B* **2000**, *104*, 11805−11815.

(34) Kwa, S. L. S.; Newell, W. R.; van Grondelle, R.; Dekker, J. P. *Biochim. Biophys. Acta* **1992**, *1099*, 193−202.

(35) Alfonso, M.; Montoya, G.; Cases, R.; Rodriguez, R.; Picorel, R. *Biochemistry* **1994**, *33*, 10494−10500.

(36) Dekker, J. P.; Bowlby, N. R.; Yocum, C. F. *FEBS Lett.* **1989**, *254*, 150−154.

(37) Groot, M. L.; Peterman, E. J. G.; van Stokkum, I. H. M.; Dekker, J. P.; van Grondelle, R. *Biophys. J.* **1995**, *68*, 281−290.

(38) Eijckelhoff, C.; Dekker, J. P. *Biochim. Biophys. Acta* **1995**, *1231*, 21−28.

(39) Gradinaru, C. C.; van Stokkum, I. H. M.; Pascal, A. A.; van Grondelle, R.; van Amerongen, H. *J. Phys. Chem. B* **2000**, *104*, 9330−9342.

(40) Wilhelm, T.; Piel, J.; Riedle, E. *Opt. Lett.* **1997**, *22*, 1494−1496.

(41) van Stokkum, I. H. M.; Scherer, T.; Brouwer, A. M.; Verhoeven, J. W. *J. Phys. Chem.* **1994**, *98*, 852−866.

(42) Groot, M. L.; Peterman, E. J. G.; van Kan, P. J. M.; van Stokkum, I. H. M.; Dekker, J. P.; van Grondelle, R. *Biophys. J.* **1994**, *67*, 318−330.

(43) Durrant, J. R.; Giorgi, L. B.; Barber, J.; Klug, D. R.; Porter, G. *Biochim. Biophys. Acta* **1990**, *1017*, 167−175.

(44) Yruela, I.; van Kan, P. J. M.; Müller, M. G.; Holzwarth, A. R. *FEBS Lett.* **1994**, *339*, 25−30.

(45) Renge, I.; van Grondelle, R.; Dekker, J. P. *J. Photochem. Photobiol.* **1996**, *96*, 109−121.